Partially Folded Conformations in the Folding Pathway of Bovine Carbonic Anhydrase II: A Fluorescence Spectroscopic Analysis

Natalia A. Bushmarina,[a] Irina M. Kuznetsova,[a] Alexander G. Biktashev,[a] Konstantin K. Turoverov,*[a] and Vladimir N. Uversky*[b]+

GdmCl-, urea-, and pH-induced unfolding pathways of bovine carbonic anhydrase II have been analyzed by using changes induced by different denaturing agents in intensity, anisotropy, life time, and parameter A *value of intrinsic fluorescence as well as intensity and life time of ANS (ammonium salt of 8-anilinonaphthalene-1-sulfonic acid) fluorescence. The formation of several stable unfolding intermediates, some of which were not observed previously, has been established. This was further confirmed by representation of fluorescence data in terms of a "phase diagram", that is,* $I_{\lambda 1}$ *versus* $I_{\lambda 2}$ *dependence, where* $I_{\lambda 1}$ *and* $I_{\lambda 2}$ *are the fluorescence intensity values measured at wavelengths* λ_1 *and* λ_2*, respectively.*

KEYWORDS:

carbonic anhydrase · fluorescence spectroscopy · intermediates · lyases · protein folding

Introduction

Carbonic anhydrase (CA, carbonate hydro-lyase, carbonate dehydratase, EC 4.2.1.1) is a zinc-containing enzyme catalyzing with high efficiency the reversible hydration of carbon dioxide:

$$CO_2 + H_2O \longrightarrow HCO_3^- + H^+$$

This reaction, underlying many diverse physiological processes in animals, plants, archaebacteria, and eubacteria, may be effectively inhibited by various substances including different monovalent anions (for example bisulfite, formate, cyanate, azide, sulfate, etc.), sulfonamides, phenol, imidazole, triazole, and specific proteinacous CA inhibitors.[1] CA is an ubiquitous enzyme found in human, all animals, and photosynthesizing organisms examined for its presence. It was also discovered in some non-photosynthetic bacteria.[1]

There are three evolutionary unrelated CA families, designated as α, β, and γ, whose representatives, all being zinc enzymes, show slight sequence homology.[2] Thus, CA families represent a good example of convergent evolution of catalytic function.[1] All known carbonic anhydrases from animals belong to the α-CA family. α-CA was also found in a few bacteria[2] and in the unicellular green alga *Chlamydomonas reinardtii*.[3] However, no α-CA has been found in higher plants. On the contrary, β-CAs have been shown to be present in higher plants[4] and in several bacteria.[2] Only one member of the γ-CA family, CA of the methanogenic archaebacterium *Methanosarcina thermophila*, has been isolated to date.[5]

CAs isolated from the same species show a large heterogeneity determined both genetically and by "conformational" modifications (for example by deamidation[6] or glycosylation[7]). In fact, seven genetically distinct α-CA isozymes, with sequence length varying from 259 to 312 amino acid residues, have been identified in mammalians. These isozymes are encoded by genes located on four different chromosomes.[1] Isozymes have different tissue distributions and intracellular locations, being cytoplasmic or membrane-bound. For example, human CA I is the major non-hemoglobin protein of red cells, which is also found in a number of other tissues, such as the colon, but is not as widely distributed as CA II,[8] which is the most studied form. CA I is also less active than CA II.[9] CA II has an exceptionally high CO_2 hydration turnover.[9] This isozyme is traditionally purified from red cells. However, it has a wide tissue distribution and is found in many different organs and cell types.[8] All CA isozymes are essentially different with respect to catalytic efficiency and inhibitor-binding properties.

[a] *Prof. K. K. Turoverov, N. A. Bushmarina, Dr. I. M. Kuznetsova, A. G. Biktashev*
Institute of Cytology
Russian Academy of Sciences
Tikhoretsky Ave. 4, 194064 St. Petersburg (Russia)
Fax: (+7) 812-247-0341
E-mail: kkt@mail.cytspb.rssi.ru

[b] *Dr. V. N. Uversky*+
Department of Chemistry and Biochemistry
University of California
Santa Cruz, CA 95064 (USA)
Fax: (+1) 831-459-2935
E-mail: uversky@hydrogen.ucsc.edu

[+] *Further address:*
Institute for Biological Instrumentation
Russian Academy of Sciences
142292 Pushchino, Moscow Region (Russia)

There is an essential pharmacological interest in CA because it was shown that this enzyme is the target for drugs, such as acetazolamide, methazolamide, dichlorphenamide,[1] and the recently developed dorzolamide[10] for the treatment of glaucoma. This is because carbonic anhydrase inhibitors, both topical and systemic, lower intraocular pressure by reducing HCO_3^- formation in the ciliary process, thus lowering Na^+ transport and the flow of aqueous humor.[11]

The crystal structures of human CA I and II, CA II from the Indian buffalo, bovine CA III, and a truncated form of murine CA V have been determined.[12] The overall structures of these isozymes are very similar. The molecules are nearly spherical with approximate dimensions of $5 \times 4 \times 4$ nm^3. With the exception of ca. 25 N-terminal amino acid residues, which are loosely connected to the rest of the molecule, these α-CAs have been considered as single-domain proteins. The preponderant secondary structure is a ten-stranded, twisted β sheet, which is mostly antiparallel. A few relatively short helices are located on the surface of the molecule, and α-CAs have been classified as α/β proteins.[13]

Thus, α-CAs belong to the class of single-domain proteins with predominant β structure. It has been shown that these proteins (and particularly human CA II and bovine CA B, or CA II) are ideally suited for the investigation of the mechanisms of folding and unfolding of a polypeptide chain.[14] – [18] This is especially the case for bovine carbonic anhydrase II, BCA II, as this protein contains no cysteine or cystine residues, thus allowing unfolding studies to focus exclusively on the successive conformational changes without complications from sulfhydryl oxidation and disulfide formation. As a result, the equilibrium unfolding of BCA II induced either by pH,[15] urea,[17] or guanidinium hydrochloride (GdmCl)[14, 17, 18] has been intensively studied. It was shown that the equilibrium unfolding pathway of BCA II is characterized by the presence of several intermediate states. A molten-globule state is accumulated at around pH 3.6,[15] or at neutral pH and room temperature in the presence of moderate GdmCl concentrations.[14, 17] At low temperatures, GdmCl-induced unfolding of BCA II is characterized by the formation of two partially folded conformations, the molten-globule state and its precursor.[18]

In the present study we introduce fluorescence spectroscopic measurements that further characterize the process of BCA II unfolding induced by pH, urea, or GdmCl. To this end, changes induced by different denaturing agents in intrinsic fluorescence parameters (intensity, maximum position, anisotropy, life time, and parameter *A* value) or ANS (ammonium salt of 8-anilinonaphthalene-1-sulfonic acid) fluorescence parameters (intensity, maximum position, and life time) are studied. In addition, the method of "phase diagrams" is applied to fluorescence data analysis. The essence of this method is to construct the diagram $I_{\lambda 1}$ versus $I_{\lambda 2}$, where $I_{\lambda 1}$ and $I_{\lambda 2}$ are the fluorescence intensity values measured at wavelengths λ_1 and λ_2, respectively. This approach allows us to describe the unfolding pathway of BCA II in much detail and to detect the formation of several stable unfolding intermediates, some of which have not been observed previously.

Results and Discussion

GdmCl-induced equilibrium unfolding and refolding of BCA II

GdmCl-induced unfolding: Figures 1 and 2 show that the fluorescence behavior of BCA II during the GdmCl-induced equilibrium unfolding or refolding is a complex process. Figure 1 depicts GdmCl dependencies of intrinsic fluorescence intensities

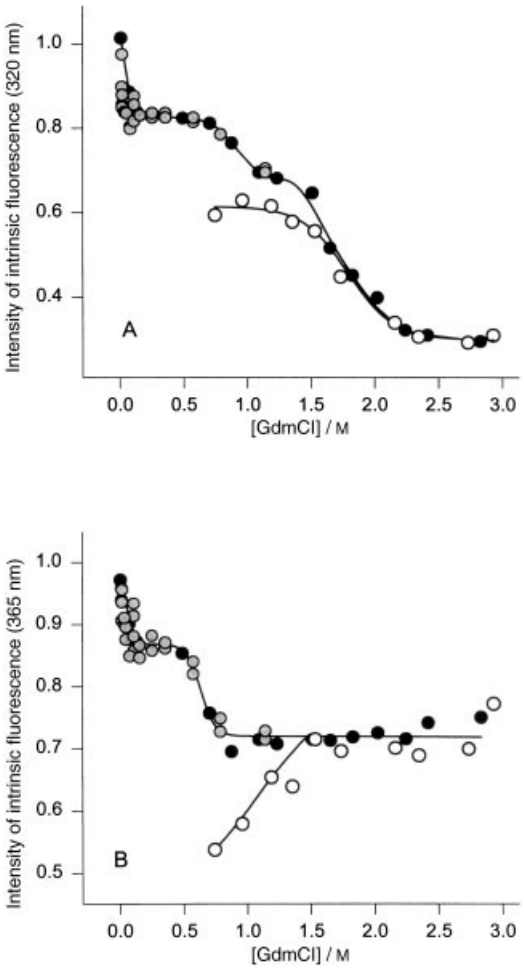

Figure 1. *GdmCl-induced changes in BCA II intrinsic fluorescence intensity at $\lambda =$ 320 nm, I_{320} (A), and $\lambda = 365$ nm, I_{365} (B). Fluorescence was excited at 297 nm. Black circles correspond to the unfolding experiments. Open and gray circles correspond to the refolding experiments, which were initiated from 6.0 M or 1.2 M GdmCl, respectively. Protein concentration was 0.1 mg mL^{-1}. All measurements were carried out at 23 °C.*

measured at $\lambda_{em} = 320$ nm (Figure 1 A) and $\lambda_{em} = 365$ nm (Figure 1 B). One can see that the fluorescence intensities decrease with an increase in GdmCl concentration in a rather complex manner. An initial drop of both intensities takes place within an extremely narrow interval of denaturant concentrations (between 0 and 0.1 M GdmCl), which is accompanied by a rather extended plateau followed by a further sigmoidal decrease. The changes in fluorescence intensity are completed at ca. 2.5 and ca. 1.0 M GdmCl for I_{320} and I_{365}, respectively. This means that GdmCl-induced unfolding of BCA II (i.e. transition from the native, N, to the unfolded state, U) is characterized by the

formation of at least two equilibrium intermediate conformations, I_1^{GdmCl} and I_2^{GdmCl}, which are populated at around 0.1 and 1.0 M GdmCl respectively.

Figure 2 represents GdmCl-induced changes in parameter *A*, in the anisotropy of intrinsic fluorescence, and in the intensity of ANS fluorescence. Figure 2A shows that between 0 and 0.1 M GdmCl the parameter *A* value ($A = I_{320}/I_{365}$, which is characteristic of the shape and position of the fluorescence spectrum[19]) decreases. Soon after, this parameter starts to increase and reaches a maximum at ca. 1.1 M GdmCl. However, a further increase in denaturant concentration leads to a pronounced decrease in the parameter *A* value, which is finished at ca. 2.5 M GdmCl. As for the anisotropy of the intrinsic fluorescence, this parameter gradually increases between 0 and ca. 1.6 M GdmCl. In the range of 1.6 – 3.0 M GdmCl, there is an essential decrease in the anisotropy value, which reflects the unfolding of the protein (see Figure 2A). Thus, data on the GdmCl dependence of the anisotropy reflect an accumulation of the third intermediate, I_3^{GdmCl}, maximally populated at around 1.6 M GdmCl. Higher anisotropy values characteristic of this intermediate may reflect lower intramolecular mobility of tryptophan residues or protein association.

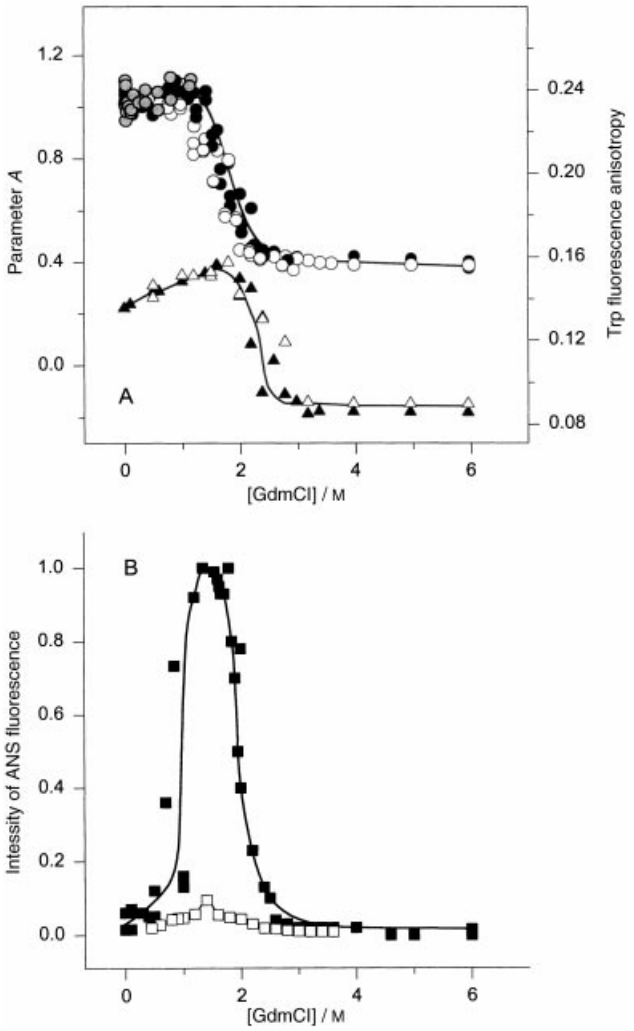

Figure 2. *A: GdmCl-induced changes in the intrinsic fluorescence of BCA II. The circles represent parameter* A *[$(I_{320}/I_{365})_{297}$], the triangles the degree of Trp fluorescence anisotropy (*r*). Fluorescence was excited at 297 nm, the protein concentration was 0.1 mg mL^{-1}. B: GdmCl-induced changes in ANS fluorescence intensity in the presence of BCA II. Protein and ANS concentrations were 0.1 and 0.02 mg mL^{-1}, respectively. Fluorescence was excited at 350 nm. Black symbols correspond to the unfolding experiments. Open and gray symbols correspond to the refolding experiments, which were initiated from 6.0 M or 1.2 M GdmCl, respectively. All measurements were carried out at 23 °C.*

Changes in ANS fluorescence intensity are frequently used to monitor formation of partially folded intermediates during protein unfolding and refolding.[20] The reason is that the presence of large solvent-exposed hydrophobic patches is a general property of a partially folded protein molecule. The interaction of ANS with such exposed hydrophobic clusters in a protein is accompanied by a considerable increase in the dye fluorescence intensity and a pronounced blue shift of the fluorescence maximum. Figure 2B shows that an increase in GdmCl concentration is accompanied by essential changes in the intensity of ANS fluorescence. One can see that this parameter reaches a maximal value at 1.5 – 1.8 M GdmCl, confirming the appearance of an intermediate I_3^{GdmCl} containing the solvent-exposed hydrophobic surfaces.

Figure 3 also confirms the idea that GdmCl-induced unfolding of BCA II is an exceptionally complex process. This picture was designed by using the method of "phase diagrams" elaborated by Burstein for the analysis of fluorescence data.[21] It has been shown that such an approach is extremely sensitive to the accumulation of any intermediate state.[21, 22]

Figure 3 clearly shows that the phase diagram plotted for the GdmCl-induced unfolding of BCA II consists of three linear parts, corresponding to 0 – 0.1, 0.1 – 1.0 and 1.0 – 6.0 M GdmCl concentration. This reflects the existence of three independent transitions: $N \leftrightarrow I_1^{GdmCl}$, $I_1^{GdmCl} \leftrightarrow I_2^{GdmCl}$, and $I_2^{GdmCl} \leftrightarrow U$. Interestingly, neither studies of parameter *A* nor representing data on the GdmCl dependence of intrinsic fluorescence intensity in terms of a phase diagram allows the detection of the I_3^{GdmCl} intermediate (populated at around 1.6 M GdmCl). However, accumulation of this intermediate is accompanied by an extensive increase in ANS fluorescence intensity and the pronounced rise of the intrinsic fluorescence anisotropy (see Figure 2). This illustrates the importance of the multiparametric approach to the analysis of conformational transformations in proteins.

The insensitivity of parameter *A* and phase diagram to the formation of the I_3^{GdmCl} intermediate may be explained assuming that three conformations, I_2^{GdmCl}, I_3^{GdmCl}, and U, coexist within 1.0 – 2.5 M GdmCl. The value of parameter *A* that characterizes the shape and position of the fluorescence spectrum for I_3^{GdmCl} is an intermediate between those measured for I_2^{GdmCl} and U (not shown). This makes I_3^{GdmCl} "invisible" for approaches dealing with the characteristics of the intrinsic fluorescence spectrum (parameter *A* and phase diagram).

I_1^{GdmCl} intermediate: Interestingly, a small increase in GdmCl concentration is already accompanied by measurable changes of BCA II fluorescence parameters. In fact, our data are consistent with the appearance of the first intermediate state, I_1^{GdmCl}, at around 0.1 M GdmCl, that is, well before a noticeable change of

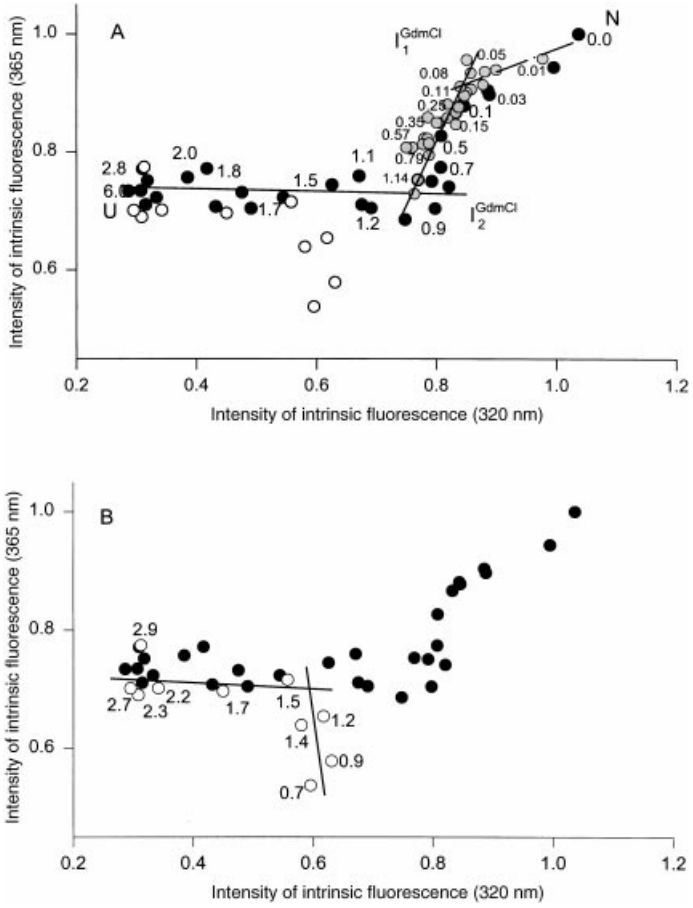

Figure 3. *Phase diagrams representing unfolding (A) and refolding of BCA II induced by GdmCl (B). Black circles correspond to the unfolding experiments. Open and gray circles correspond to the refolding experiments, which were initiated from 6.0 M or 1.2 M GdmCl, respectively. Concentrations of denaturant are indicated next to the respective symbol. Each straight line represents an all-or-none transition between two conformers, denoted as N, I_1^{GdmCl}, I_2^{GdmCl}, I_3^{GdmCl}, and U.*

any other structural parameter takes place. The effect of small denaturant concentrations on the activity of enzymes was intensively studied over the last decade.[23, 24] It has been reported that changes in enzyme activity may occur before essential changes of the enzyme molecule as a whole can be detected. This observation has been interpreted in terms of the relative weakness of interactions involved in the stabilization of enzyme active sites.[24] Our results show for the first time that activity is not the only enzyme characteristic that may be affected by low GdmCl concentrations.

Equilibrium unfolding intermediates I_2^{GdmCl} and I_3^{GdmCl}: The nature of the I_3^{GdmCl} intermediate is certain—it is the molten-globule state. Earlier, a combination of several spectroscopic and hydrodynamic techniques revealed that GdmCl-induced equilibrium unfolding of BCA II at room temperature is accompanied by the formation of the molten-globule state, that is, a compact denatured intermediate.[14, 17] The molten globule is accumulated at 1.5 – 1.8 M GdmCl,[14, 17] that is, at denaturant concentrations where the appearance of the I_3^{GdmCl} intermediate was detected.

Figure 1 shows that a large part of the fluorescence intensity of the native enzyme is lost around 1.0 M GdmCl, that is, under conditions favoring accumulation of the I_2^{GdmCl} intermediate. It has been demonstrated for the structurally homologous human CA II that, due to energy transfer and quenching effects, the quantum yields and λ_{max} vary considerably for the different Trp residues in the native state, but these differences almost disappeared upon denaturation and partial unfolding.[16d] However, it has been established earlier that BCA II possesses native-like near- and far-UV CD spectra[14b, 18] and even native-like activity under these denaturing conditions.[14a, 18] This allows us to assume that significant changes in the fluorescence intensity in this case could still represent only small conformational rearrangements, and I_2^{GdmCl} may be considered as the native-like intermediate.

To better understand the origin of the equilibrium unfolding intermediates I_2^{GdmCl} and I_3^{GdmCl}, data on BCA II refolding kinetics may be considered. The refolding kinetics of this protein have been studied by a variety of methods over a wide time range (from milliseconds to hours).[25] It has been shown that this process proceeds through three stages. In the first stage, solvent-exposed hydrophobic clusters and a compact state of the polypeptide chain are formed. In the second stage, hydrophobic clusters are desolvated and a rigid native-like hydrophobic core is formed. During the third stage the native state is formed.[25] In other words, kinetic data revealed the accumulation of two intermediates, the molten globule and essentially native-like ones. We are assuming that I_3^{GdmCl} and I_2^{GdmCl} intermediates resemble the molten-globule and native-like intermediates observed in the kinetic pathway of BCA II refolding. The accumulation of the native-like intermediate, I_2^{GdmCl}, in the equilibrium unfolding of BCA II is described here for the first time.

Time-resolved measurements of ANS fluorescence: Figure 4 represents ANS fluorescence decay curves measured for the native state (Figure 4 A) and the I_3^{GdmCl} equilibrium intermediate accumulated at around 1.5 M GdmCl (Figure 4 B). It can be seen that the longest component of fluorescence decay for the ANS – native protein complex is characterized by $\tau = 11.8 \pm 0.5$ ns, whereas in the presence of 1.5 M GdmCl a ca. 1.25-fold increase in this value is observed ($\tau = 13.7 \pm 0.5$ ns).

This observation confirms the assumption that I_3^{GdmCl} is the compact denatured conformation. It is known that the fluorescence decay of free ANS has an uni-exponential character, whereas the formation of ANS – protein complexes yields at least a double-exponential fluorescence decay.[26] In this case the shorter lifetime component of the fluorescence decay ($\tau < 6$ ns) is characteristic of the dye molecules that interact with the surface of a protein molecule, while the longer lifetime component ($\tau > 10$ ns) refers to the protein-embedded ANS molecules.[26] The good correlation between changes in the longest lifetime component and overall conformational changes of the protein molecule was shown. The value of this parameter is sensitive to whether ANS interacts either with the native (N) or with the compact denatured (D) protein molecule ($\tau_N \leq 12$ ns as compared with $\tau_D \geq 14$ ns).[26]

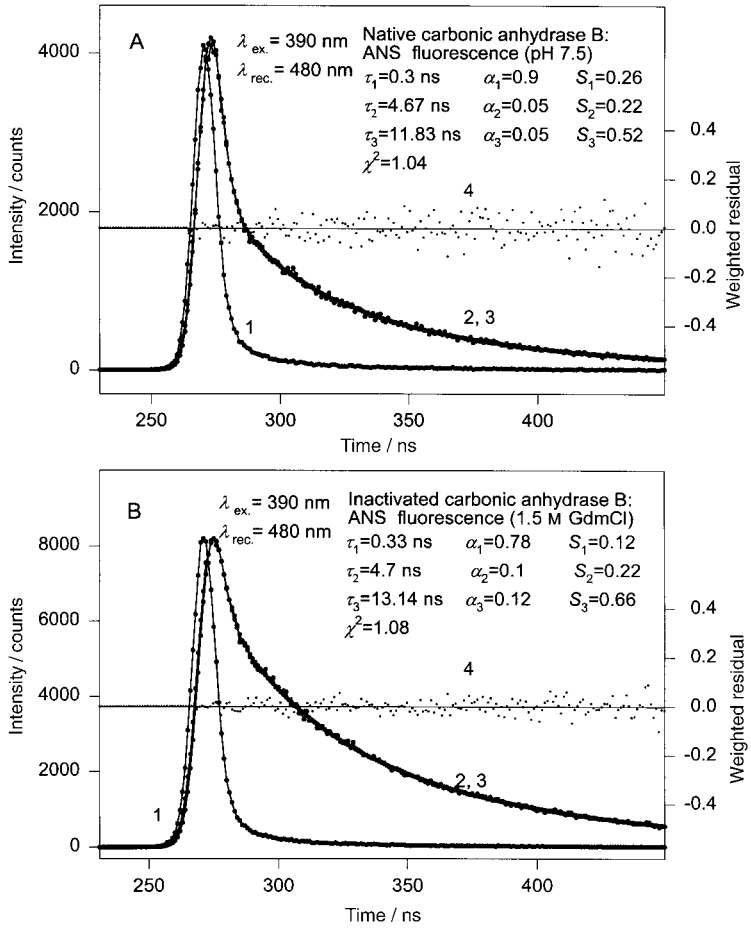

Figure 4. *ANS fluorescence decay curves measured for native BCA II (A) and its I_3^{GdmCl} intermediate (B). The figures represents the excitation lamp profile (curve 1), the experimental decay curve (curve 2), the best-fit calculated fluorescence decay curve (curve 3), and the deviation between the experimental and the calculated decay curves (weighted residuals; curve 4). The protein/ANS molar ratio was 1:20. The protein concentration was 1.0 mg mL^{-1}. The excitation wavelength was 390 nm, the recording wavelength was 480 nm. All measurements were carried out at 23 °C.*

Equilibrium refolding of BCA II from concentrated GdmCl solutions: Let us now consider the data concerning the equilibrium refolding of BCA II from concentrated GdmCl solutions (6 M GdmCl; see open symbols in Figures 1 – 3). The results presented in Figure 2 A may be interpreted in terms of complete reversibility of BCA II unfolding. However, Figures 1 and 3 clearly show that Trp fluorescence intensities, I_{365} and I_{320}, are not restored completely upon the decrease in GdmCl concentration. Moreover, ANS fluorescence intensity in at 1.5 – 1.8 M GdmCl is lower during refolding (Figure 2 B). This means that in diluted GdmCl solutions (below 1.0 M) only a relatively small fraction of BCA II molecules is refolded successfully, whereas the majority of protein precipitates when BCA II refolds from 6 M GdmCl. This conclusion is in good agreement with the recent study of BCA II refolding by quasi-elastic light scattering.[27] In fact, the efficiency of BCA II refolding from 5 M GdmCl was strongly dependent on the final denaturant and protein concentrations. Below 1.0 M GdmCl the majority of the protein molecules formed large aggregates even though the final protein concentration was as low as 0.1 mg mL^{-1}.[27]

Reversible equilibrium refolding of BCA II from 1.2 M GdmCl solutions: Interestingly, the situation is completely different when BCA II refolding is initiated from moderate GdmCl concentrations, as represented by the gray symbols in Figures 1 – 3. These figures represent data on the equilibrium refolding studies, in which the process was initiated by dilution of BCA II from a 1.2 M GdmCl solution. One can see that the first two transitions, $N \leftrightarrow I_1^{GdmCl}$ and $I_1^{GdmCl} \leftrightarrow I_2^{GdmCl}$, are completely reversible in these experiments. This means that contrary to the I_3^{GdmCl} conformer, formation of I_1^{GdmCl} and I_2^{GdmCl} intermediates are not accompanied by protein association, at least at the BCA II concentrations studied (ca. 0.1 mg mL^{-1}).

Urea-induced equilibrium unfolding and refolding of BCA II

Contrary to the GdmCl-induced unfolding experiments, we were unable to detect any intermediate during the unfolding of BCA II by urea (cf. ref. [17]). In fact, we have established that between 0 and ca. 5.5 M urea the protein remains in its native state. Further increase in denaturant concentration (from 5.5 to 6.5 M) leads to the complete unfolding of the protein, detected by a decrease in the anisotropy happening simultaneously with the decrease in the parameter *A* values (data not shown). Moreover, there is no characteristic increase in the ANS fluorescence intensity within the studied range of urea concentrations (from 0.0 to 8.0 M). Finally, urea-induced changes (if any) in all studied fluorescence parameters were completely reversible (data not shown).

Effect of pH on BCA II fluorescence characteristics

Decrease in pH: The most complex picture was observed for the pH-induced structural transformations of BCA II (see Figures 5 – 7). Figure 5 depicts pH dependencies of I_{320} and I_{365}. One can see that as the pH decreases, both parameters decrease initially and have a sharp minimum at around pH 4.2. A further decrease in pH leads to an increase in fluorescence intensities whose maximal values are around pH 3.6. Finally, between pH 3.2 and 3.0 there is an additional decrease in I_{320} and I_{365}.

Figure 6 A represents the pH dependencies of parameter *A* and of the anisotropy of intrinsic fluorescence. This figure shows that between pH 6 and 4.5 parameter *A* is unchanged. As the pH decreases parameter *A* reaches a maximum at pH ~ 4.0. There is a pronounced plateau between pH 4.0 and 3.2, followed by an decrease in parameter *A*. This takes place within a narrow pH interval (from pH 3.2 to 3.0). A further decrease in pH is not accompanied by changes in the parameter *A* value. The anisotropy of intrinsic fluorescence increases between pH 4.5 and 4 and then gradually decreases until it almost reaches the value for the native state. The effect of pH decrease on ANS fluorescence intensity is shown in Figure 6 B. One can see that this parameter has a maximal value at around pH 3.6.

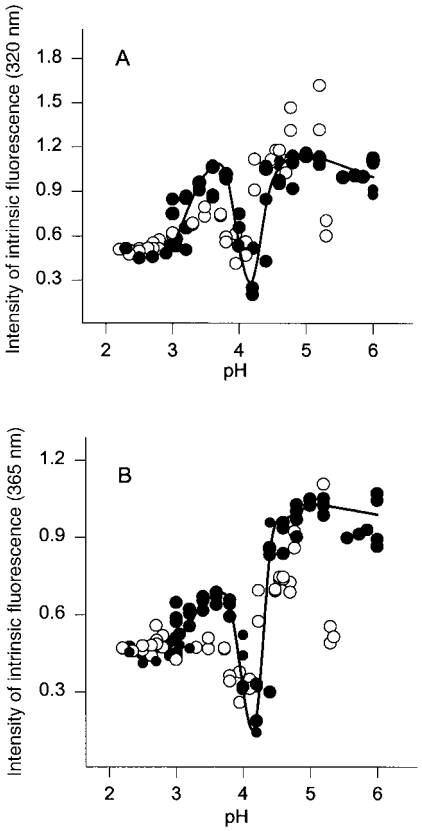

Figure 5. *Changes in BCA II intrinsic fluorescence intensity at $\lambda = 320$ nm, I_{320} (A), and $\lambda = 365$ nm, I_{365} (B) induced by changes in pH value. Fluorescence was excited at 297 nm. Black and open circles correspond to the unfolding and refolding experiments, respectively. The protein concentration was 0.1 mg mL^{-1}. All measurements were carried out at 23 °C.*

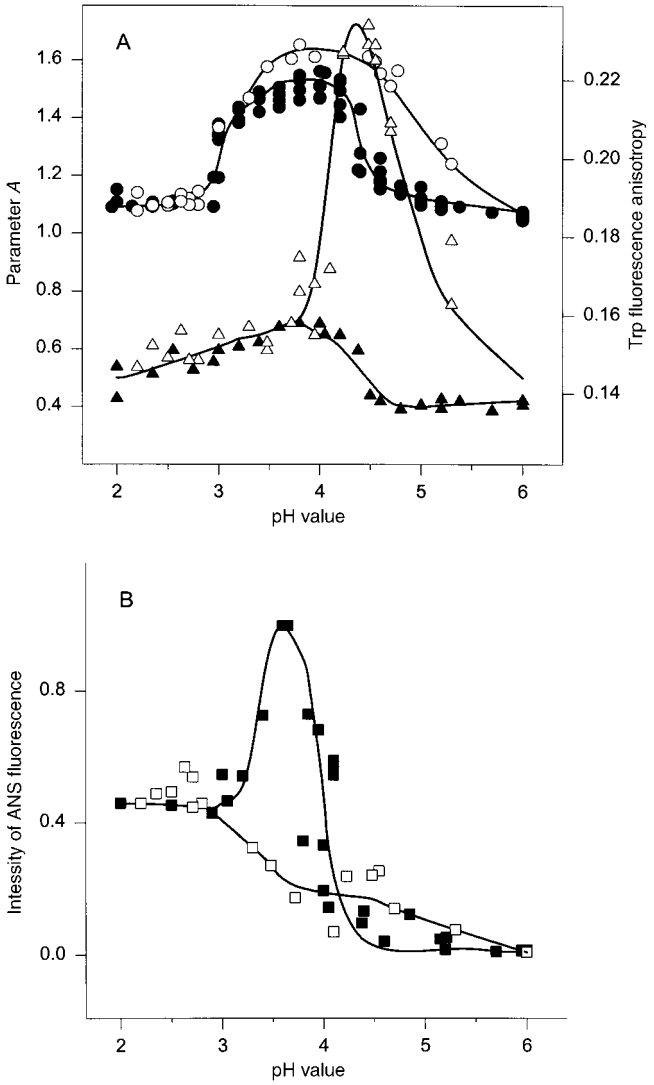

Figure 6. *A: Changes in intrinsic fluorescence of BCA II induced by changes in pH value. $A = (I_{320}/I_{365})_{297}$ (circles), degree of intrinsic fluorescence anisotropy, r (triangles). Fluorescence was excited at 297 nm. Protein concentration was 0.1 mg mL^{-1}. B: Changes in ANS fluorescence intensity in the presence of BCA II induced by changes in pH value. Protein and ANS concentrations were 0.1 and 0.02 mg mL^{-1}, respectively. Fluorescence was excited at 350 nm. Black and open symbols correspond to the unfolding and refolding experiments, respectively. All measurements were carried out at 23 °C.*

Interestingly, data presented in Figures 5 and 6 show that BCA II is not completely unfolded even at extremely low pH. In fact, at pH 2.0 parameter *A* and the anisotropy of intrinsic fluorescence have native-like values. Moreover, under these conditions ANS fluorescence intensity is relatively high (ca. 1/2 of its maximal value).

Intramolecular mobility of tryptophan residues: The mobility of the tryptophan residues can be estimated from fluorescence anisotropy measurements. We have established that the transition of BCA II from the native to the intermediate state is accompanied by a considerable increase in the fluorescence anisotropy value *r*. Such an increase in fluorescence anisotropy may be due to the decrease in the internal mobility of tryptophan residues, or/and protein association.

Figure 7 represents Perrin plots ($1/r$ versus T/η dependencies) for the native (pH 7.5), compact partially folded (pH 3.6), and completely unfolded BCA II in the presence of 8 M urea. It can be seen that the slope of $1/r$ versus T/η dependence for the native protein is essentially larger than for the partially folded BCA II. This may reflect the association of partially folded BCA II molecules. In order to analyse these dependencies in more detail, the fluorescence decay curves were measured for native (pH 7.5) and partially folded BCA II (pH 3.6). The fluorescence decay plot of the native protein shows bi-exponential character, whereas three components are present in the fluorescence decay plot of partially unfolded BCA II (data not shown). The mean-square values of the fluorescence life time were determined to be equal to 4.5 and 3.3 ns for native BCA II and the pH-3.6 intermediate, respectively. This gives 34 and 70 ns for ρ_{exp}, the rotational relaxation time. The rotational relaxation time of the equivalent sphere, ρ_0, is equal to 46 ns. The rotational relaxation time of the tryptophan residue intramolecular mobility (ρ_{IMM}) was evaluated from Equation (11) (see Materials and Methods) and found to be about 130 ns. Thus, though there is an intramolecular mobility of tryptophan residues in native BCA II, the dependence of $1/r$ vs. T/η is mainly determined by the overall rotational motion of the macromolecule. Furthermore, compar-

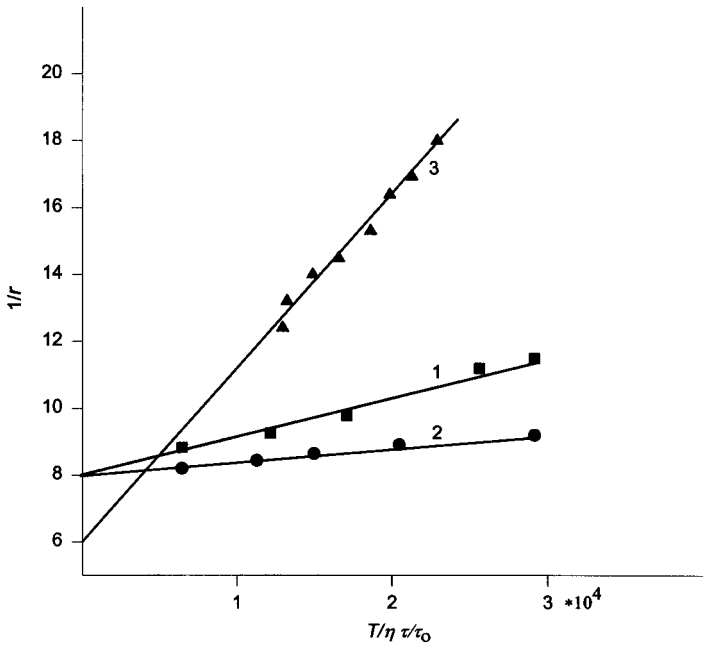

Figure 7. Perrin plots (1/r versus T/η dependence) for different conformational states of BCA II: 1, native protein (pH 7.5); 2, pH-3.6 intermediate; 3, completely unfolded protein in the presence of 8 M urea. The excitation wavelength was 297 nm. The recording wavelength of fluorescence anisotropy was 365 nm. The solvent viscosity η was varied by changing the water/glycerol ratio. All measurements were carried out at a protein concentration of 0.5 mg mL^{-1} and a temperature of 23 °C.

ison of ρ_{exp} and ρ_0 shows that the tryptophan residues in native BCA II participate in the intramolecular mobility on the nanosecond time scale, that these motions are dependent on solvent viscosity, and also that the pH-3.6 intermediate is a dimer.

Further analysis of Figure 7 shows that the value of the intercept cut by the Perrin plot on the *y* axis ($1/r'_0$) for both the native BCA II and the pH-3.6 intermediate is equal to 8.0 ± 0.2. This exceeds the corresponding value for low molecular weight model compounds, such as *N*-acetyltryptophan, for which $1/r'_0 = 5.4 \pm 0.2$. Therefore, in these two conformations the tryptophan residues participate in the high-frequency intramolecular motions whose rotational relaxation time is much shorter than the lifetime of the excited state.[28] Alternatively, these tryptophan residues may be involved in the intramolecular mobility on the nanosecond time scale whose rotational relaxation time does not depend on solvent viscosity.[29] Finally, the fact that $1/r'_{0\,p.f.} = 1/r'_{0native}$ (p.f. = partially folded) indicates that the amplitude of the high-frequency motions or the rotational relaxation time for the intramolecular mobility on the nanosecond time scale, whose rotational relaxation time does not depend on the solvent viscosity, or both, are comparable in partially folded and native BCA II.

Reversibility of pH-induced changes in BCA II: Open circles in Figures 5 and 6 represent results of the experiments on the equilibrium refolding of BCA II from the acid-unfolded conformation (pH 2.0). These data show that changes in BCA II fluorescence parameters are reversible only within the pH range 2.0 – 3.0. A further increase in pH is characterized by an essential discrepancy in the behavior of all studied parameters. Remarkably, there is a large increase in Trp fluorescence anisotropy at pH 4.5 – 4.6. All this may be due to the aggregation of partially folded protein molecules.

Thus, our data on the fluorescence spectroscopic analysis of BCA II unfolding illustrate the diversity of unfolding pathways for a given protein at room temperature. In fact, the unfolding process of BCA II may represent an "all-or-none" $N \leftrightarrow U$ transition, as observed for urea-induced unfolding. However, it may also be more complex and involve accumulation of two (pH-induced unfolding) or three partially folded intermediates (GdmCl-induced unfolding). Interestingly, although the unfolding behavior of BCA II has been studied for several decades,[15–18] the formation of several intermediates, I_1^{GdmCl}, I_2^{GdmCl}, and I_1^{pH}, is described here for the first time. Obviously, further structural characterizations of these intermediates and the acid-unfolded state of BCA II are required.

Materials and Methods

Fluorescence spectroscopic measurements: Fluorescence spectroscopic experiments were carried out in spectrofluorimeters with the steady state and impulse excitation.[30] Fluorescence was excited at the long-wave absorption edge where the contribution of tyrosine residues is negligible. Fluorescence intensity was recorded at 320 and 365 nm. The position and form of the fluorescence spectra were characterized by the parameter $A = (I_{320}/I_{365})_{297}$, where I_{320} and I_{365} are fluorescence intensities at $\lambda_{em} = 320$ and 365 nm, respectively, and $\lambda_{ex} = 297$ nm.[19] In some cases the whole spectrum was recorded. The values of parameter *A* and of the fluorescence spectrum were corrected by the instrument sensitivity. ANS fluorescence was excited at 390 nm and recorded at 480 nm.

Phase diagram method: The method of phase diagrams was elaborated by Burstein for fluorescence data analysis.[21] The essence of this approach is to construct the diagram of $I_{\lambda 1}$ versus $I_{\lambda 2}$, where $I_{\lambda 1}$ and $I_{\lambda 2}$ are the fluorescence intensity values measured at wavelengths λ_1 and λ_2 under the different experimental conditions for a protein undergoing structural transformations. As fluorescence intensity is the extensive parameter, it will describe any two-component system by a simple relationship [Eq. (1)].

$$I(\lambda) = \alpha_1 I_1(\lambda) + \alpha_2 I_2(\lambda) \quad (1)$$

$I_1(\lambda)$ and $I_2(\lambda)$ are the fluorescence intensities of the first and second components, respectively, whereas α_1 and α_2 are their relative contents ($\alpha_1 + \alpha_2 = 1$). Excluding α_1 ($\alpha_1 = 1 - \alpha_2$), Equation (1) could be rewritten as:

$$I(\lambda) = (1\text{-}\alpha_2) I_1(\lambda) + \alpha_2 I_2(\lambda) = I_1(\lambda) + \alpha_2 (I_2(\lambda) - I_1(\lambda)) \quad (2)$$

It is obvious that α_2 may be determined from the fluorescence intensity measurements at two different wavelengths, λ_1 and λ_2 [Eq. (3) and (4)]. Thus

$$I(\lambda_1) = I_1(\lambda_1) + \alpha_2 (I_2(\lambda_1) - I_1(\lambda_1)) \quad (3)$$

$$I(\lambda_2) = I_1(\lambda_2) + \alpha_2 (I_2(\lambda_2) - I_1(\lambda_2)) \quad (4)$$

and

$$\alpha_2 = \frac{I(\lambda_2) - I_1(\lambda_2)}{I_2(\lambda_2) - I_1(\lambda_2)}. \quad (5)$$

This allows determination of the relationship between $I(\lambda_1)$ and $I(\lambda_2)$ by substitution of α_2 in Eq. (3) with the expression in Eq. (5), yielding Equation (6),

$$\begin{aligned} I(\lambda_1) &= I_1(\lambda_1) + \frac{I(\lambda_2) - I_1(\lambda_2)}{I_2(\lambda_2) - I_1(\lambda_2)}(I_2(\lambda_1) - I_1(\lambda_1)) \\ &= I_1(\lambda_1) - \frac{I_2(\lambda_1) - I_1(\lambda_1)}{I_2(\lambda_2) - I_1(\lambda_2)} I_1(\lambda_2) + \frac{I_2(\lambda_1) - I_1(\lambda_1)}{I_2(\lambda_2) - I_1(\lambda_2)} I(\lambda_1) \end{aligned} \quad (6)$$

or Equation (7),

$$I(\lambda_1) = a + b\, I(\lambda_2) \quad (7),$$

with a and b defined by Equations (8) and (9).

$$a = I_1(\lambda_1) - \frac{I_2(\lambda_1) - I_1(\lambda_1)}{I_2(\lambda_2) - I_1(\lambda_2)} I_1(\lambda_2) \quad (8)$$

$$b = \frac{I_2(\lambda_1) - I_1(\lambda_1)}{I_2(\lambda_2) - I_1(\lambda_2)}. \quad (9)$$

When applied to protein unfolding, Equation (7) predicts that the dependence $I(\lambda_1) = f(I(\lambda_2))$ will be linear if changes in protein environment lead to the all-or-none transition between two different conformations. On the contrary, the nonlinearity of this function reflects the sequential character of structural transformations. Moreover, each linear portion of the $I(\lambda_1) = f(I(\lambda_2))$ dependence will describe the individual all-or-non transition.

Analysis of the fluorescence decay: To analyze the decay curves a special program was elaborated. The fitting routine was based on the nonlinear least-squares method. Minimization was accomplished according to Marquardt.[31] *P*-Terphenyl in ethanol and *N*-acetyltryptophanamide in water were used as reference compounds.[32] Experimental data were analyzed with a multiexponential approach [Eq. (10)],

$$I(t) = \sum_i \alpha_i \exp(-t/\tau_i) \quad (10),$$

where α_i and τ_i are amplitude and lifetime of component i, respectively; $\sum_i \alpha_i = 1$.

Evaluation of intramolecular mobility: The rotational relaxation time of the intramolecular mobility (ρ_{IMM}) of tryptophan was evaluated on the basis of the experimentally determined relaxation time (ρ_{exp}) and the calculated value for a rigid macromolecule (ρ_0) according to Equation (11).[33]

$$\frac{1}{\rho_{exp}} = \frac{1}{\rho_0} + \frac{1}{\rho_{IMM}} \quad (11)$$

The rotational relaxation time of a rigid sphere with a volume equivalent to that of a protein is defined by Equation (12)

$$\rho_0 = \frac{3\eta M}{RT}\left(1 + \frac{\omega}{\nu d}\right) \quad (12),$$

where η is the solvent viscosity, M the molecular weight, R the gas constant, T the absolute temperature, ω the hydration coefficient, $\bar{\nu}$ the specific partial volume, and d the specific solution density. The limits of the ρ_0 variation due to the molecular ellipticity were evaluated on the basis of the data given in ref. [29].

The rotational relaxation time ρ_{exp} was evaluated on the basis of the Perrin plot [Eq. (13)],

$$\frac{1}{r} = \frac{1}{r_0'}\left(1 + \frac{RT}{V\eta}\langle\tau\rangle\right) = \frac{1}{r_0'}\left(1 + 3\frac{\langle\tau\rangle}{\rho_{exp}}\right) \quad (13),$$

where r is the fluorescence anisotropy, r_0' the intercept cut by the Perrin plot on the y axis, V the effective volume of the protein macromolecule, and $\langle\tau\rangle$ the root-mean square value of the fluorescence lifetimes. The biexponential decay can be expressed by Equation (14).

$$\langle\tau\rangle = \frac{\alpha_1\tau_1^2 + \alpha_2\tau_2^2}{\alpha_1\tau_1 + \alpha_2\tau_2} \quad (14)$$

Unfolding of BCA II induced by GdmCl and urea: The protein was dissolved in 50 mM Tris buffer (pH 7.5) for the unfolding experiments. Small aliquots of this stock solution were added to the reaction mixture containing the desired concentrations of urea or GdmCl. Before measurements, these protein solutions were incubated for 40 h at room temperature to reach equilibrium.

Refolding of BCA II induced by GdmCl and urea: Experiments on the denaturant-induced equilibrium refolding have been performed as follows. Initially, the protein was dissolved in 50 mM Tris buffer (pH 7.5) containing 6.0 M (or 1.2 M) GdmCl or 8 M urea. These stock solutions were incubated for 24 h. Then small aliquots of the stock solutions were added to the reaction mixture containing the desired concentrations of GdmCl or urea. The resulting protein solutions were incubated for 40 h at room temperature to reach equilibrium prior to measurements.

Unfolding and refolding of BCA II induced by pH changes: Experiments on the pH-induced unfolding and refolding of BCA II were performed in 50 mM Gly-HCl (pH range from 2.0 to 3.6, buffer A) or 100 mM sodium citrate/citric acid (pH range from 3.0 to 6.0, buffer B) buffer systems. Desired pH values were adjusted by using 0.1 M NaOH or HCl. The protein was dissolved and incubated for 24 h in buffer A or B for the unfolding or refolding experiments, respectively. Small aliquots of concentrated protein stock solutions were added to the reaction mixture having the desired pH value. The resulting protein solutions were incubated for 40 h at room temperature to reach equilibrium prior to measurements.

We are grateful to M. Hokenson for the careful reading and editing of the manuscript. This work was supported by grant Nos. 00-04-49224 and 00-15-97824 from the RFBR, RFBR-NSFC grant No. 99-04-39106, and NATO grant LST.CLG 975190.

[1] S. Lindskog, *Pharmacol. Ther.* **1997**, *74*, 1 – 20.
[2] D. Hewett-Emmett, R. E. Tashian, *Mol. Phylogenet. Evol.* **1996**, *5*, 50 – 77.
[3] a) H. Fukuzawa, S. Fujiwara, Y. Yamamoto, M. L. Dionisio-Sese, S. Miyachi, *Proc. Natl. Acad. Sci. USA* **1990**, *87*, 4383 – 4387; b) J. Karlsson, T. Hiltonen, H. D. Husic, Z. Ramazanov, G. Samuelsson, *Plant. Physiol.* **1995**, *109*, 533 – 539.
[4] M. R. Badger, G. D. Price, *Annu. Rev. Plant Physiol.* **1994**, *45*, 369 – 392.
[5] B. E. Alber, J. G. Ferry, *Proc. Natl. Acad. Sci. USA* **1994**, *91*, 6909 – 6913.
[6] M. Bouthier, J. M. Gulian, B. Mallet, R. Calaf, J. Reynaud, *Biochimie* **1979**, *61*, 1161 – 1168.
[7] A. Waheed, X. L. Zhu, W. S. Sly, *J. Biol. Chem.* **1992**, *267*, 3308 – 3311.
[8] W. S. Sly, P. Y. Hu, *Annu. Rev. Biochem.* **1995**, *64*, 375 – 401.
[9] R. G. Khalifah, *J. Biol. Chem.* **1971**, *246*, 2561 – 2573.

[10] a) T. H. Maren, C. W. Conroy, *J. Biol. Chem.* **1993**, *268*, 26233 – 26239; b) T. H. Maren, *J. Glaucoma* **1995**, *4*, 49 – 62.
[11] T. H. Maren, *Annu. Rev. Physiol.* **1988**, *50*, 695 – 717.
[12] a) A. Liljas, K. K. Kannan, P. C. Bergstén, I. Waara, K. Fridborg, B. Strandberg, U. Carlbom, L. Järup, S. Lövgren, M. Petef, *Nat. New. Biol.* **1972**, *235*, 131 – 137; b) K. K. Kannan, B. Notstrand, K. Fridborg, S. Lövgren, A. Ohlsson, M. Petef, *Proc. Natl. Acad. Sci. USA* **1975**, *72*, 51 – 55; c) V. Kumar, K. K. Kannan, R. Chidambaram, *Curr. Sci.* **1989**, *58*, 344 – 348; d) A. E. Eriksson, A. Liljas, *Proteins* **1993**, *16*, 29 – 42; e) P. A. Boriack-Sjodin, R. W. Heck, P. J. Laipis, D. N. Silverman, D. W. Christianson, *Proc. Natl. Acad. Sci. USA* **1995**, *92*, 10949 – 10953.
[13] J. S. Richardson, *Adv. Protein Chem.* **1981**, *34*, 167 – 339.
[14] a) A. Yazgan, R. W. Henkens, *Biochemistry* **1972**, *11*, 1314 – 1318; b) K. P. Wong, C. Tanford, *J. Biol. Chem.* **1973**, *248*, 8518 – 8523; c) R. W. Henkens, B. B. Kitchell, S. C. Lottich, P. J. Stein, T. J. Williams, *Biochemistry* **1982**, *21*, 5918 – 5923.
[15] a) K. P. Wong, L. M. Hamlin, *Biochemistry* **1974**, *13*, 2678 – 2683; b) D. A. Dolgikh, L. V. Abaturov, E. V. Brazhnikov, Yu. O. Lebedev, Yu. N. Chirgadze, O. B. Ptitsyn, *Dokl. Akad. Nauk SSSR* **1983**, *272*, 1481 – 1484.
[16] a) U. Carlsson, L. E. Henderson, S. Lindskog, *Biochim. Biophys. Acta* **1973**, *310*, 376 – 387; b) B. P. Ko, A. Yazgan, P. L. Yeagle, S. C. Lottich, R. W. Henkens, *Biochemistry* **1977**, *16*, 1720 – 1725; c) L. G. Mårtensson, B. H. Jonsson, P. O. Freskgård, A. Kihlgren, M. Svensson, U. Carlsson, *Biochemistry* **1993**, *32*, 224 – 231; d) L. G. Mårtensson, P. Jonasson, P. O. Freskgård, M. Svensson, U. Carlsson, B. H. Jonsson, *Biochemistry* **1995**, *34*, 1011 – 1021; e) L. F. McCoy, Jr., K. P. Wong, *Biopolymers* **1979**, *18*, 2893 – 2904; f) L. F. McCoy, E. S. Rowe, K. P. Wong, *Biochemistry* **1980**, *19*, 4738 – 4743; g) P. J. Stein, R. W. Henkens, *J. Biol. Chem.* **1978**, *253*, 8016 – 8018; h) M. Svensson, P. Jonasson, P. O. Freskgård, B. H. Jonsson, M. Lindgren, L. G. Mårtensson, M. Gentile, K. Borén, U. Carlsson, *Biochemistry* **1995**, *34*, 8606 – 8620.
[17] N. A. Rodionova, G. V. Semisotnov, V. P. Kutyshenko, V. N. Uversky, I. A. Bolotina, V. E. Bychkova, O. B. Ptitsyn, *Mol. Biol (Moscow)* **1989**, *23*, 683 – 692.
[18] V. N. Uversky, O. B. Ptitsyn, *J. Mol. Biol.* **1996**, *255*, 215 – 228.
[19] K. K. Turoverov, B. V. Shchelchkov, *Biofizika* **1970**, *15*, 965 – 972.
[20] G. V. Semisotnov, N. A. Rodionova, O. I. Razgulyaev, V. N. Uversky, A. F. Gripas', R. I. Gilmanshin, *Biopolymers* **1991**, *13*, 119 – 128.
[21] "Intrinsic Protein Fluorescence: Origin and Applications": E. A. Burstein in *Biophysics*, *Vol. 7*, VINITI, Moscow, **1976**.
[22] E. A. Permyakov, V. V. Yarmolenko, V. I. Emelyanenko, E. A. Burstein, C. Gerday, J. Closset, *Eur. J. Biochem.* **1980**, *109*, 307 – 315.
[23] a) Q. Z. Yao, H.-M. Zhou, L. X. Hou, C.-L. Tsou, *Sci. Sin. [B]* **1982**, *26*, 1296 – 1302; b) Q. Z. Yao, M. Tian, C.-L. Tsou, *Biochemistry* **1984**, *23*, 2740 – 2744; c) G. F. Xie, C.-L. Tsou, *Biochim. Biophys. Acta* **1987**, *911*, 19 – 24; d) W. Liu, C.-L. Tsou, *Biochim. Biophys. Acta* **1987**, *916*, 455 – 464; e) L. Y. Chen, M. Tian, J. S. Du, M. Ju, *Biochim. Biophys. Acta* **1990**, *1039*, 61 – 66; f) S. M. West, S. M. Kelly, N. C. Price, *Biochim. Biophys. Acta* **1990**, *1037*, 332 – 336; g) S. J. Liang, Y. Z. Lin, J. M. Zhou, C.-L. Tsou, P. Q. Wu, Z. M. Zhou, *Biochim. Biophys. Acta* **1990**, *1038*, 240 – 246; h) S. M. Kelly, N. C. Price, *Biochem. J.* **1991**, *275*, 745 – 749; i) Y. Z. Ma, C.-L. Tsou, *Biochem. J.* **1991**, *277*, 207 – 211.
[24] a) C.-L. Tsou, *Trends Biochem. Sci.* **1984**, *11*, 427 – 429; b) H.-M. Zhou, X.-H. Zhang, Y. Yin, C.-L. Tsou, *Biochem. J.* **1993**, *291*, 103 – 107.
[25] G. V. Semisotnov, N. A. Rodionova, V. P. Kutyshenko, B. Ebert, J. Blank, O. B. Ptitsyn, *FEBS Lett.* **1987**, *224*, 9 – 13.
[26] a) V. N. Uversky, S. Winter, G. Löber, *Biophys. Chem.* **1996**, *60*, 79 – 88; b) V. N. Uversky, S. Winter, G. Löber, *Biochim. Biophys. Acta* **1998**, *1388*, 133 – 142.
[27] J. L. Cleland, D. I. C. Wang, *Biochemistry* **1990**, *29*, 11072 – 11078.
[28] I. M. Kuznetsova, S. Yu. Khaitlina, S. N. Konditerov, A. M. Surin, K. K. Turoverov, *Biophys. Chem.* **1988**, *32*, 73 – 78.
[29] I. M. Kuznetsova, K. K. Turoverov, *Mol. Biol. (Moscow)* **1983**, *17*, 741 – 754.
[30] K. K. Turoverov, A. G. Biktashev, A. V. Dorofeyuk, I. M. Kuznetsova, *Tsitologiya* **1998**, *40*, 806 – 817.
[31] D. W. Marquardt, *J. Soc. Ind. Appl. Math.* **1963**, *11*, 431 – 441.
[32] M. Zuker, A. G. Szabo, L. Bramall, D. T. Krajcarski, B. Selinger, *Rev. Sci. Instrum.* **1985**, *56*, 14 – 22.
[33] E. V. Anufrieva, Yu. Ya. Gotlib, M. G. Krakovyak, S. S. Skorokhodov, *Vysokomol. Soedin. Ser. A* **1972**, *14*, 1430 – 1450.

Received: January 26, 2001
Revised version: June 1, 2001 [F 188]